

# Polymer Implants for Intratumoral Drug Delivery and Cancer Therapy

BRENT D. WEINBERG,<sup>1</sup> ELVIN BLANCO,<sup>2</sup> JINMING GAO<sup>2</sup>

<sup>1</sup>Department of Biomedical Engineering, Case Western Reserve University, 10900 Euclid Ave, Cleveland, Ohio 44106

<sup>2</sup>Simmons Comprehensive Cancer Center, University of Texas Southwestern Medical Center at Dallas, 5323 Harry Hines Blvd., Dallas, Texas 75390

Received 26 January 2007; accepted 17 April 2007

Published online in Wiley InterScience (www.interscience.wiley.com). DOI 10.1002/jps.21038

**ABSTRACT:** To address the need for minimally invasive treatment of unresectable tumors, intratumoral polymer implants have been developed to release a variety of chemotherapeutic agents for the locoregional therapy of cancer. These implants, also termed “polymer millirods,” were designed to provide optimal drug release kinetics to improve drug delivery efficiency and antitumor efficacy when treating unresectable tumors. Modeling of drug transport properties in different tissue environments has provided theoretical insights on rational implant design, and several imaging techniques have been established to monitor the local drug concentrations surrounding these implants both *ex vivo* and *in vivo*. Preliminary antitumor efficacy and drug distribution studies in a rabbit liver tumor model have shown that these implants can restrict tumor growth in small animal tumors (diameter <1 cm). In the future, new approaches, such as three-dimensional (3-D) drug distribution modeling and the use of multiple drug-releasing implants, will be used to extend the efficacy of these implants in treating larger tumors more similar to intractable human tumors. © 2007 Wiley-Liss, Inc. and the American Pharmacists Association *J Pharm Sci* 97:1681–1702, 2008

**Keywords:** biodegradable polymers; imaging methods; cancer chemotherapy; drug transport; controlled release; mathematical model; drug targeting

## INTRODUCTION

Cancer is an enormous health concern in the United States and in recent years has surpassed heart disease as the predominant cause of death for all but the most elderly Americans.<sup>1</sup> Currently, the most curative treatment option for solid tumors is surgical resection followed by adjuvant

chemotherapy or radiation therapy to minimize the risk of recurrence. Many cancers respond well to this treatment strategy, but many patients are not eligible for surgical resection. For example, out of 70000 newly diagnosed colon cancer metastases to the liver in the US per year, the number of patients who are actually candidates for surgery is disappointingly low at 2500–4500.<sup>2</sup> Reasons limiting resection include tumor size, involvement of more than one liver lobe, or a co-existing liver condition (e.g., cirrhosis).<sup>2,3</sup> In addition, the overall survival rates for these patients even after surgery are often low.<sup>4</sup> Other

Correspondence to: Jinming Gao (Telephone: 214-648-9278; Fax: 214-648-0264; E-mail: jinming.gao@utsouthwestern.edu)

*Journal of Pharmaceutical Sciences*, Vol. 97, 1681–1702 (2008)

© 2007 Wiley-Liss, Inc. and the American Pharmacists Association

abdominal cancers, such as those of the pancreas and stomach, also have low resection rates and poor overall patient survival.<sup>1</sup> Intravenously administered chemotherapy for these tumors also has limited effectiveness. Since only a small amount of the systemic blood flow is directed to the tumor, only a fraction of the total dose reaches the tumor site.<sup>5</sup> The remainder of the dose is distributed throughout healthy organs and tissues, leading to a variety of undesirable side effects ranging from neutropenia to cardiomyopathy.<sup>6,7</sup> Many chemotherapeutic drugs also have very rapid plasma clearance, leading to short tumor exposure times.<sup>8</sup> To improve the outcome of these cancer patients, a new paradigm of minimally invasive and locoregional cancer therapies has rapidly evolved and received considerable attention in the recent years.<sup>9</sup>

Image-guided, minimally invasive techniques for therapeutic interventions use regional tumor destruction as an alternative to surgical resection.<sup>10</sup> Strategies for tumor ablation include thermal heating,<sup>11,12</sup> cryosurgery,<sup>13,14</sup> or chemical ablation.<sup>15,16</sup> In each of these techniques, an interventional needle or electrode is inserted into the tumor with image guidance.<sup>17,18</sup> Then, the ablation is applied to destroy the tumor and a surrounding margin of normal tissue. Since they can be applied percutaneously, these minimally invasive treatments typically are viable alternatives to surgery that can be used in patients with poor overall health as an outpatient procedure. Additionally, local administration of the treatment maximizes destruction to the tumor target while limiting damage to the surrounding normal tissue. Ablation has been used for the treatment of several unresectable cancers, including those in the liver,<sup>19</sup> prostate,<sup>20</sup> and lung.<sup>21</sup>

Other attempts to improve treatment of unresectable tumors have focused on means to increase the tumor specificity of chemotherapeutic drugs through locoregional delivery.<sup>22</sup> Administering an anticancer drug either to the region that contains a tumor or directly within the tumor has the advantage of increasing tumor exposure to a drug while limiting systemic toxicity. One strategy for locoregional chemotherapy is to infuse a solution of a chemotherapeutic agent into the region of the malignancy. Intravesicular chemotherapy has become a common treatment for bladder tumors, and has been shown to be associated with a reduced tumor recurrence rate after surgery.<sup>23</sup> Local chemotherapy infusion has also been used with some success in the case of

advanced nonsmall cell lung cancer when patients have a malignant pleural effusion.<sup>24</sup> Additionally, several studies have shown significant benefits in treating ovarian cancers with intraperitoneal (IP) infusions.<sup>25</sup> All of these treatments require that malignant cells be in close contact with the surrounding space to which the chemotherapy is administered.

For tumors that are not externally accessible, local perfusion, or the administration of a chemotherapeutic agent to a segment of the circulation that preferentially perfuses the tumor, is an alternative. Intra-arterial administration of drugs can maximize drug delivery to blood vessels supplying tumors. For example, transarterial chemoembolization (TACE) benefits from the fact that most hepatocellular carcinomas (HCCs) receive the vast majority of their blood supply from their hepatic artery while normal liver receives its blood supply largely from the portal vein.<sup>26</sup> In this treatment, a catheter is selectively placed in the branches of the hepatic artery which feed the tumor. Once arterial selection has been achieved, a solution of chemotherapeutic agents dissolved in an oily solvents followed by embolic agents is infused into the artery.<sup>26</sup> This approach has been shown to increase concentrations of chemotherapy in the tumor by 10- to 100-fold<sup>26</sup> and to improve 1-year survival of patients with unresectable HCC by as much as 20%.<sup>27</sup> As a result, TACE has become a commonly administered therapy for unresectable HCC.<sup>28</sup> Another strategy to improve delivery is through regional perfusion, in which the portion of the systemic circulation containing a tumor is isolated from the rest of the circulation.<sup>29</sup> Isolated thoracic perfusion (ITP) is achievable by closing off the descending aorta and vena cava with balloon catheters, blocking blood flow to the arms with inflated cuffs, and introducing chemotherapy into the right atrium. This approach has been used to increase the concentration of chemotherapy delivered to lung cancers by 6- to 10-fold,<sup>30</sup> and an analogous approach exists for isolated abdominal perfusion. Each of these locoregional chemotherapy methods had been shown to increase tumor exposure to drug while reducing systemic toxicity.

Intratumoral cancer treatments extend the locoregional treatment concept by attempting to further limit the scope of chemotherapy exposure. Treatments that have been studied extensively include intratumoral infusions, injections, and implantable devices that deliver either

chemotherapeutic drugs or other therapeutic agents.<sup>22</sup> Infusion of chemotherapeutic agents has been heavily studied in the area of brain tumors, where it has spawned a field known as convection-enhanced delivery (CED).<sup>31</sup> In CED, a microcatheter is inserted into a tumor and the therapeutic agent is slowly administered to the surrounding tissue using positive pressure infusion. Major advantages of CED to brain tumors include bypassing the blood–brain barrier and delivering drugs further from the infusion site due to convection.<sup>32</sup> CED has been used to deliver conventional chemotherapeutic drugs<sup>33</sup> but has shown considerable promise for the delivery of targeted bacterial toxins<sup>31</sup> and therapeutic antibodies.<sup>34</sup> Intratumoral injections of therapeutic solutions have also shown success in treating tumors in locations other than the brain, such as the lung,<sup>35</sup> pancreas,<sup>36</sup> and liver.<sup>37</sup> Several studies have been performed in an attempt to determine optimal parameters for injection and to determine which tumor features, such as collagen content, contribute to the extent of drug delivery.<sup>38,39</sup> Furthermore, recent studies have shown that using intratumoral injection to deliver viral gene therapy vectors minimizes nonspecific expression of gene products.<sup>40,41</sup> Since intratumorally injected liquids may distribute irregularly and be cleared quickly, several investigators have introduced injectable drug depots to prolong the extent of drug release. Examples of intratumoral depots include PLGA,<sup>42–44</sup> alginate,<sup>45</sup> and albumin<sup>46</sup> microspheres as well as injectable gels which solidify upon intratumoral injection.<sup>47–49</sup> Injectable depots have the advantage of easy administration and prolonged tumor drug exposure.

Intratumoral, drug-releasing implants are a subset of the intratumoral drug delivery paradigm and have shown increasing promise in recent years. Driven by developments for the treatment of prostate<sup>50,51</sup> and brain cancers,<sup>52,53</sup> implantable devices containing either radioactive elements or chemotherapeutic drugs have become viable treatment options. The only clinically approved chemotherapeutic implant for cancer treatment is the Gliadel wafer, a carmustine(BCNU)-eluting implant fabricated from a polyanhydride copolymer, 1,3-bis-(p-carboxyphenoxy) propane/poly(sebacic acid) (pCPP:SA).<sup>54</sup> These implants were designed to treat glioblastoma multiforme, an aggressive brain cancer with extremely limited patient survival, through placement in the surgical cavity after primary surgical resection.

After placement, the implants release their drug load over a period of approximately 5 days,<sup>55</sup> and drug has been shown to penetrate several millimeters into the brain parenchyma.<sup>56</sup> A recent long-term study showed that the Gliadel implant placement after surgery increased patient survival to 13.8 months versus 11.6 months for control and maintained this survival advantage for at least 3 years after initial treatment.<sup>57</sup> Despite the clinical success of the Gliadel implant, the use of chemotherapeutic implants has yet to become widespread in the treatment of other cancers, such as those of the pancreas, liver, or lungs. However, it is likely that future chemotherapeutic implants can be optimized for use in a variety of different tumors to maximize patient comfort and survival.

This review article describes work in extending the use of intratumoral implants to treat unresectable liver tumors. The proposed treatment strategy is primary treatment of the tumor bulk with radiofrequency (RF) ablation followed by the placement of drug-eluting polymer implants in the ablated tumor region. These biodegradable polymer millirods have been fabricated from poly(D,L-lactide-co-glycolide) (PLGA) to deliver chemotherapeutic agents through and beyond the RF ablated tumor, thus maximizing tumor destruction and reducing the risk of tumor recurrence. The first section describes the overall goals that must be considered when developing any local delivery device, including the use of models to predict local drug transport. The second section describes techniques for measuring local drug concentrations and the use of these measurements to customize drug release. In the third section, this review describes the preliminary results from using these implants to treat a rabbit liver cancer model. Finally, the last section presents some conclusions drawn from the early use of these implants and some future goals to facilitate using these implants to treat larger tumors similar to unresectable human cancers.

## OVERVIEW OF DRUG DELIVERY GOALS

### Definition of Pharmacokinetic Goals for Local Drug Delivery to Unresectable Tumors

In considering the use of an intratumoral implant for tumor treatment, it is necessary to consider the generic characteristics that would benefit the device. First, the implant should be able to

minimize shortcomings associated with systemically administered chemotherapy. Second, it should provide an optimal drug delivery profile to the tumor, which is to say that it should be able to provide effective drug concentrations to the desired region over a prolonged period of time. Third, the device should be part of a comprehensive and complete treatment strategy that is versatile and applicable in a wide range of realistic situations. Achieving these goals should maximize the treatment success of these intratumoral implants.

When delivering their drug cargo to tumors, intratumoral implants must provide an optimal drug release profile that is characterized by the ability to deliver drug to a large volume, to rapidly reach the therapeutic concentration, and to maintain the therapeutic concentration for an extended time. Previous studies have shown that limited penetration distance is one of the major restrictions on the efficacy of intratumoral treatments.<sup>55,56</sup> Any successful implant must be designed in such a way that takes into consideration ways to maximize the drug delivery distance. Additionally, the implant must provide drug to the surrounding tissue at an appropriate rate.<sup>58</sup>

A schematic of ideal drug release rates is shown in Figure 1. Consider implant A, an implant which releases drug at a constant rate somewhere above the elimination rate. While local drug concentration will slowly rise, it may take too long to reach tissue concentrations that are toxic to the surrounding cancer cells. Alternatively, implant B provides a rapid dose of chemotherapy that will quickly surpass the effective concentration. However, the release rate after the initial burst is insufficient to maintain this concentration for any extended length of time. Such a release rate is undesirable, as it could allow cancer cells to recover, perhaps even with newly acquired drug resistance.<sup>59</sup> The ideal implant, implant C, combines the best characteristics of both implants: rapid ascent to the effective concentration followed by a maintenance dose to remain at a useful drug level. While this explanation is a simplification (e.g., elimination is almost certainly not constant, etc.), it serves as an example of how different drug release rates might affect local drug concentrations. Additionally, it offers some insight on how the situation can be changed by modifying the elimination rate or therapeutic concentration. For the most part, however, local drug concentrations surrounding implants must be determined experimentally.

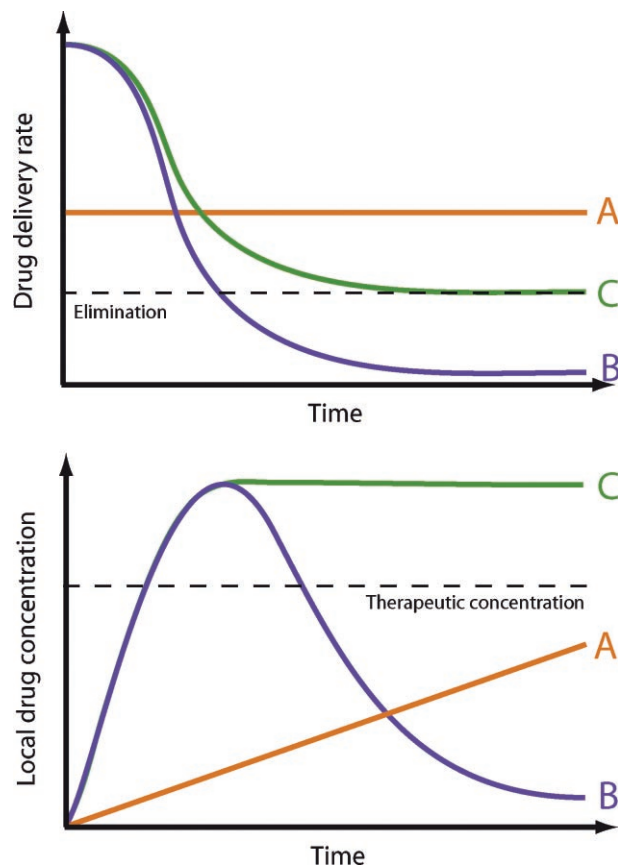


**Figure 1.** Scheme illustrating drug release and local drug concentration from three theoretical implant types. A zero-order release implant (A) releases drug at a constant rate, but it may take a long period of time to reach the therapeutic concentration. A burst-release implant (B) releases large amounts of drug early, but may not extended release to maintain a therapeutic concentration. A dual-release implant (C) combines an early burst of drug to accelerate the rise to therapeutic concentrations with sustained release to maintain therapeutic concentrations.

The success of chemotherapeutic implants for cancer treatment also depends on their inclusion in a comprehensive tumor treatment strategy. As an example, with the previously mentioned Gliadel treatment, the tumor is first surgically resected (“debulked”) followed by the placement of multiple BCNU-impregnated implants in the surgical cavity.<sup>52</sup> The design of a liver cancer treatment using polymer millirods proposes a similar strategy to Gliadel treatment: using RF ablation to destroy the majority of the tumor mass followed by placement of polymer implants in the tumor to kill any residual cancer cells and limit tumor recurrence. RF ablation is already used clinically to treat liver tumors, but tumor

recurrence, particularly around the ablation boundary, has greatly limited the clinical success of tumor ablation.<sup>60,61</sup> Using chemotherapeutic implants with ablation may maximize the benefit compared to using the implants alone. The ablation destroys the majority of the tumor cells, leaving the implants to kill only the remaining cells, thereby reducing the risk of recurrence. Furthermore, tumor ablation may facilitate drug delivery from the implants by changing the fundamental rates governing drug transport in the tumors.<sup>58</sup> To develop this strategy, drug-impregnated, PLGA polymer millirods with different release rates were developed and tested in animal models, first in nonablated and ablated liver tissue<sup>62–65</sup> and then in nonablated and ablated liver tumors.<sup>66,67</sup> Results from these studies are described in “Measuring and Modulating Local Drug Pharmacokinetics” and “Treatment of Animal Tumor Models Sections.”

#### Interstitial Drug Transport Models in Tumor and Surrounding Tissues

In addition to generic considerations on drug release from implants, the mechanisms of drug transport and elimination in the surrounding tumor tissue have a major effect on how an implant delivers drug to the tumor.<sup>68</sup> Drug released locally into the tumor has several possible fates that will ultimately affect the outcome of the treatment. Primarily, drug molecules can either move to another location through a transport process or be eliminated such that they no longer exert their desired effect.

Drug can typically be transported by two mechanisms: diffusion and convection.<sup>55,69,70</sup> In diffusion, free drug moves from a region of higher drug concentration to an adjacent region of lower drug concentration at a rate proportional to the concentration gradient. Diffusion is a primary mode of transport, particularly when drug is being released from a local implant. Convection, on the other hand, is the transport of drug along with the bulk flow of a fluid. In organs that have a high rate of interstitial fluid flow, convection is especially important. Convection also has a significant role in the flow of systemically administered chemotherapeutic agents from the vascular space to the tumor, where it travels along the same flow that delivers nutrients to the tumor.<sup>68</sup> The relative importance of diffusion or convection in drug transport depends on the delivery system

and tissue type. For instance, in the brain, where interstitial fluid constantly flows from the ventricles to the surrounding parenchyma, convection has a significant effect on the extent of drug penetration.<sup>71</sup> In situations with small molecular drugs where flow is more limited, diffusion is the predominant mode of drug transport.

Drug elimination can occur through several different mechanisms. One route of drug elimination is through metabolism. Once in a cell, drug can be altered or bound in a variety of ways. Some drug molecules, such as 5-fluorouracil, bind irreversibly to their therapeutic target, after which they are no longer in the population of available drug.<sup>72</sup> More generally, cells have a variety of nonspecific methods for detoxification, such as organelles for breaking down foreign molecules through enzymatic or pH-mediated degradation. Alternatively, cells contain protective molecules, such as glutathione, which are designed specifically to bind foreign molecules and render them more hydrophilic and less potent.<sup>73</sup> Either of these metabolic pathways essentially inactivates the drug. When considering implantable drug delivery systems, another mechanism of drug loss is perfusion away from the target region.<sup>58</sup> In this situation, drug is transported by either diffusion or convection into one of two systemic circulations, the blood or the lymph. The vasculature is a fast-moving circulation which rapidly moves drugs away from the target region and into other parts of the body. Since most chemotherapeutic agents have short plasma half-lives, once the drug reaches the plasma it is unlikely to return to the target tumor, and for practical purposes can be considered eliminated. While the lymph is a slower-moving body of fluid that can contribute to drug convection, its effects are probably less influential than those of blood because tumors are known to have limited and poorly organized lymphatic drainage.<sup>70</sup> Any drug contained in lymphatic fluid eventually moves into the venous circulation, where it undergoes the same fate as drug that directly diffuses into blood vessels.

Consider the example of drug transport shown in Figure 2, in which drug is being delivered to a liver tumor from a cylindrical implant in the center of the tumor. Previous work has shown that transport in liver can be reasonably approximated without including convection.<sup>58</sup> Drug leaving the implant is transported away from the implant into the tumor tissue based on a tumor diffusion rate,  $D_{\text{tumor}}$ . Once in the tumor, drug can be eliminated

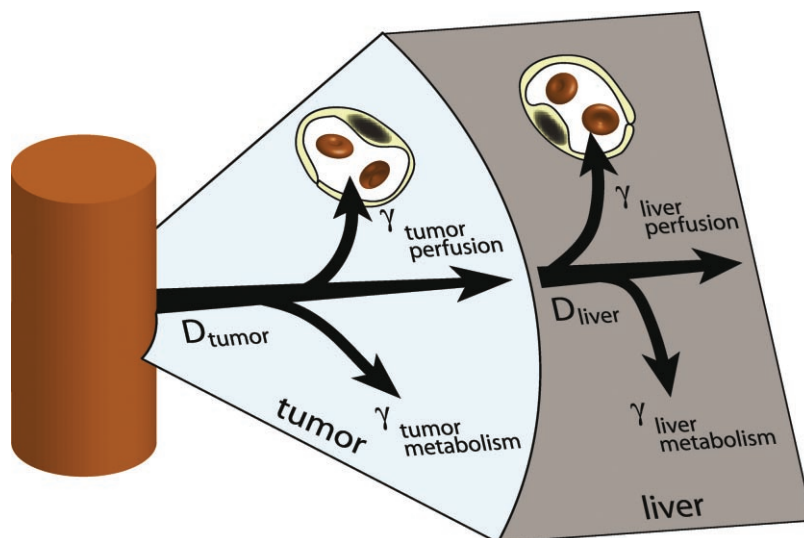


**Figure 2.** Simplified scheme of drug transport from an implant centrally placed in a liver tumor. Transport of the drug into the tumor tissue is governed by the diffusion constant of drug in tumor ( $D_{\text{tumor}}$ ), and two simultaneous modes of elimination: metabolism to inactive forms in tumor cells ( $\gamma_{\text{tumor metabolism}}$ ) or transport into nearby blood vessels which wash drug out of the region ( $\gamma_{\text{tumor perfusion}}$ ). Once drug reaches the surrounding normal tissue, it continues to diffuse outward into liver tissue ( $D_{\text{liver}}$ ), where it has different rates of elimination by metabolism ( $\gamma_{\text{liver metabolism}}$ ) or perfusion ( $\gamma_{\text{liver perfusion}}$ ).

in one of two ways, through blood flow and metabolism, proportional to two different constants which sum to contribute to a total elimination,  $\gamma_{\text{tumor}}$ . Once drug reaches the outer boundary of the tumor, it can diffuse into the surrounding normal liver tissue, where its fate is again governed by new diffusion and elimination rates. If elimination can be considered approximately first order, the drug transport in each tissue is governed by the following equation:

$$\frac{\partial C}{\partial t} = D\nabla^2 C - \gamma C \quad (1)$$

where  $C$  is the drug concentration,  $t$  the time,  $\nabla$  the gradient operator, and  $D$  and  $\gamma$  are the tissue-specific rates of diffusion and elimination, respectively. Drug transport properties in each tissue can be estimated by solving this equation computationally and minimizing the error between model output and experimentally collected data.

The use of such a model provides insight into factors that can facilitate or impede drug transport from a local implant. First, any factor that increases the rate of drug transport or lowers the rate of drug elimination will increase the permeation of drug within the tissue. For instance, some work in ex vivo tumors has shown that prolonged

drug exposure raises drug diffusion coefficients, presumably by killing cells and destroying overall structure.<sup>74</sup> Other work by Saltzman and coworkers<sup>56</sup> has shown that including high molecular weight molecules, such as dextrans, can increase transport away from implants by increasing the convective fluid flow contribution while decreasing blood perfusion. Similarly, it can be expected that any factor that reduces elimination will also have a beneficial effect, facilitating deeper drug penetration into the tumor. On the other hand, any action that decreases transport or increases elimination will act as a barrier to drug delivery that will effectively reduce the distance over which an implant can be effective. Inflammation, such as that occurring after RF ablation, may raise blood flow and decrease drug diffusion rates as a result of collagen deposition around the wound.<sup>75</sup> These side effects could certainly impede successful drug transport from a local tumor treatment. The distance at which an implant can have an effect on a tumor depends on the drug release rate from the implant as well as the balance between local transport and elimination. Unfortunately, several studies have indicated that antitumor implants are likely only effective for a few millimeters away from the implant surface.<sup>76</sup> Studies into local drug concentration

and local transport mechanisms, however, have provided useful information on ways to overcome these limitations.

## MEASURING AND MODULATING LOCAL DRUG PHARMACOKINETICS

### Overview of Methods to Investigate Local Drug Release and Tissue Distribution

In developing an intratumoral chemotherapy device, techniques for monitoring local drug concentrations are necessary to optimize implant design. Measuring drug concentration as a function of time provides a quantitative method to compare multiple treatments. Many different techniques can be used to monitor drug release from intratumoral implants. While certain techniques require extraction of tissue and measurement of drug concentration *ex vivo*, alternate, noninvasive imaging based-techniques can be used to measure concentrations *in vivo*. New implant designs or treatment conditions can be tested by creating an implant that has the ideal characteristics described in the Introduction Section; a rapid ascent to and prolonged stay above the therapeutic concentration. Additionally, drug concentration information can then be used as input to estimate tissue transport properties. Then, ideal implants can be created through a combination of empirical testing and engineering design.

Considerable information has been obtained by monitoring local drug concentrations using *ex vivo* analysis of extracted tissues. Two main categories of *ex vivo* analysis exist: bulk tissue analysis by conventional spectroscopic methods or tissue section analysis by imaging-based methods. The key principle of bulk tissue measurements is the removal of a sizeable piece of tissue followed by the use of a spectroscopic method to determine the average drug concentration in that tissue.<sup>77</sup> For targeted drug delivery to tumors, drug concentrations in different tumor regions are the most important, so these tissues are often removed in different sections. To determine tissue drug concentrations, tissues are weighed and either mechanically or chemically homogenized according to the desired detection mechanism. Examples of techniques to measure drug concentration in the extracted tissues include fluorescence detection, high performance liquid chromatography (HPLC),<sup>77,78</sup> mass spectrometry, and atomic

absorption spectroscopy (AAS).<sup>62</sup> If the drug target is radiolabeled, drug concentrations can also be measured using liquid scintigraphy. Key advantages of measuring drug concentrations in removed tissues include definitive drug detection, high sensitivity, and the ability to detect low drug concentrations. However, these techniques are restricted by low spatial resolution and accuracy, as measurements are an average over an entire piece of tissue. Achieving spatial measurements depends on the size of pieces cut from the tissue, which usually limits spatial resolution from these techniques to the millimeter range.

Imaging of *ex vivo* tissues can help overcome the spatial resolution limitations of bulk tissue analysis methods. For imaging-based methods, the tissue is removed and sliced into a thin piece followed by drug detection through imaging the slice. At least two techniques have been used for imaging drug detection: autoradiography and fluorescence.<sup>74</sup> For autoradiography, the drug target is radiolabeled and then detected by exposing the tissue section to a flat panel detector or X-ray film.<sup>56,74</sup> Advantages of this technique include high sensitivity, very low detection limits, and high resolution, while the major limitation is working with a radiolabeled drug. Fluorescent detection of drug concentration in tissues is an alternate strategy. In this method, tissue slices are analyzed using a fluorescence scanner or fluorescent microscope to detect drug.<sup>78</sup> To use this technique, the drug must either be intrinsically fluorescent or labeled with a fluorescent tag, such as fluorescein isothiocyanate (FITC).<sup>79</sup> While also offering low detection limits, reasonable sensitivity, and good resolution, only a few small molecule drugs are fluorescent, and labeling of drugs inevitably modifies their transport and efficacy, unlike radiolabeling methods. For large molecules, such as protein drugs or antibodies, fluorescent labeling may have only a minimal effect on the overall drug properties and may not adversely affect the delivery system, making the approach more tenable. *Ex vivo* drug detection is a major tool in developing local drug delivery methods, but temporal information is limited because every time point requires animal euthanasia and removal of tissue.

Noninvasive imaging methods for measuring local drug concentrations represent a growing trend in attempts to address the temporal limitations of *ex vivo* approaches. Driven by advances in imaging technology as well as proliferation of scanner availability, noninvasive

imaging methods likely hold the future for monitoring drug concentrations from local delivery strategies. With noninvasive imaging, a single subject can be imaged several times throughout the study period, greatly increasing the data available from a smaller number of animal subjects. The most straightforward extension of previous detection technologies is use of radiolabeled drugs coupled with positron emission tomography (PET)<sup>80</sup> or single photon emission tomography (SPECT) for drug detection.<sup>5</sup> These detection methods have existed clinically for several years, but recent development of specialized small animal scanners, often coupled with CT for anatomical information, has improved resolution and usability, making nuclear medicine techniques key for development of targeted therapies. Additionally, these techniques can be easily translated to clinical use for monitoring of clinical trials of newly developed devices or treatment strategies. Other imaging techniques, such as *in vivo* fluorescence imaging, have been specifically developed for use in small animals and can contribute primarily to small animal studies. With *in vivo* fluorescence imaging, fluorescently labeled molecules are imaged directly in the animal.<sup>81</sup> Most fluorescent imaging suffers from greater background noise than radiographic imaging and limitation to two dimensions, but developments in tomographic fluorescence offer the potential to reduce noise and provide three-dimensional (3-D) localization of drug.<sup>82</sup> Beyond radiolabeling and fluorescence, magnetic resonance imaging (MRI) detection of drugs or drug carriers labeled with an MRI contrast agent, such as gadolinium or superparamagnetic iron oxide (SPIO), also offers the potential to noninvasively image anatomical detail and drug concentrations simultaneously.<sup>83–85</sup> Recent advances and the benefits afforded by noninvasive imaging make it likely that these techniques will dominate the future landscape of monitoring local drug delivery strategies.

A novel noninvasive method used in the development of polymer millirods for liver cancer treatment is drug detection using X-ray computed tomography (CT).<sup>86–88</sup> Polymer implants were loaded with the anticancer drug carboplatin and tested in both normal and ablated rat liver tissue. Carboplatin has a unique property among cancer drugs in that it contains the heavy metal platinum ( $Z = 78$ ), which has high X-ray attenuation and provides inherent CT contrast. Polymer millirods containing carboplatin were implanted in non-

ablated or RF ablated rat livers, and carboplatin was detected by performing CT scans at multiple time points after implantation.<sup>88</sup> A representative CT scan of one of these rats is shown in Figure 3. Slices perpendicular to the long axis of the implant clearly show the higher absorption of the implant compared to the surrounding tissue. By comparing the intensity of the implant to premeasured implants with known concentrations, the remaining carboplatin in the implant was determined. The drug concentrations in the implants and surrounding tissue were determined by subtracting the background signal and converting to drug concentrations based on scans of

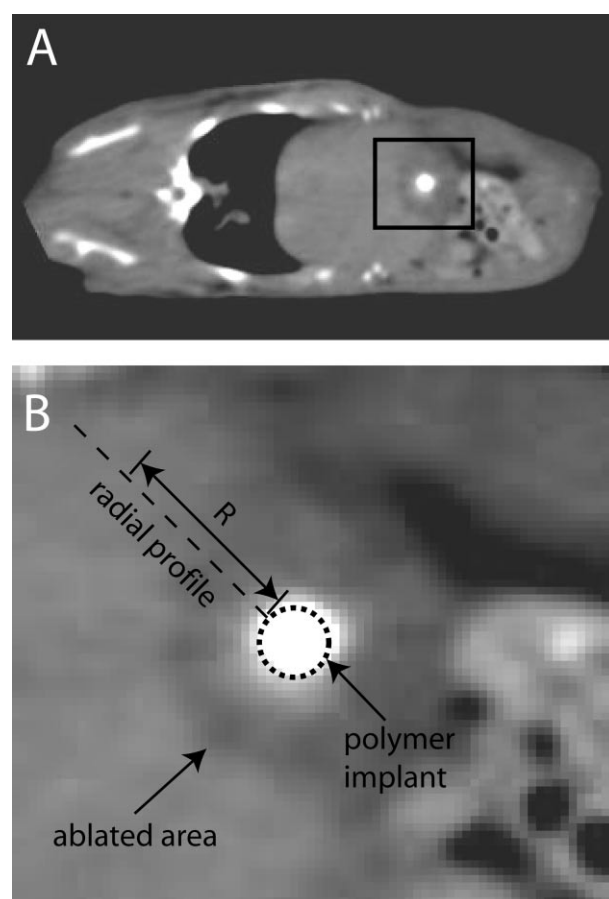


**Figure 3.** Computed tomography (CT) scan of rat with a polymer millirod containing the anticancer agent carboplatin placed in a region of liver treated by radio-frequency ablation. A: Oblique slice through the rat showing the general location of the polymer implant in the liver (black square). B: Enlargement of the implant region showing the ablated region and implant. Drug concentrations can be approximated by measuring the image intensity arising from carboplatin as a function of distance,  $R$ , from the implant surface. Adapted from Reference<sup>88</sup> with permission.



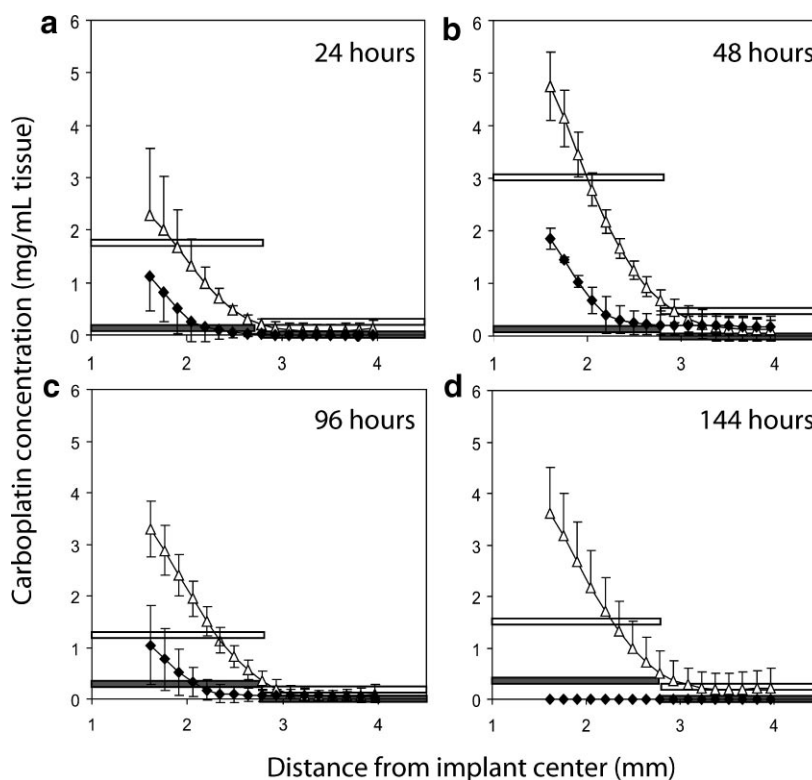


**Figure 4.** Carboplatin distribution in normal ( $\blacklozenge$ ) and ablated ( $\triangle$ ) liver tissue measured by CT. Values reflect mean  $\pm$  SD between animals. Atomic absorption spectroscopy (AAS) measurements confirm drug concentrations in tissue sections 2 mm wide from both ablated (white rectangle) and normal (gray rectangle) liver tissue. AAS data represent the average drug concentration determined over a tissue sample the width of the rectangle. Adapted from Reference<sup>88</sup> with permission.

premeasured standards. Tissue concentrations of carboplatin determined from CT images are shown in Figure 4 along with validation measurements determined using AAS of platinum concentration in extracted tissues. CT provided higher spatial resolution than AAS and revealed differences in drug distribution in nonablated and ablated tissues not appreciated by AAS. Ablated tissue retained carboplatin for longer times and at greater distances from the implant than nonablated tissue, illustrating a fundamental difference between drug transport in these tissue environments. Additionally, these results validated the use of a noninvasive imaging strategy to monitor local drug release from implants.

Further studies of local drug concentration around implants using fluorescent imaging allowed for greater quantification of the differences between ablated and normal tissue.<sup>89</sup> Doxorubicin, a topoisomerase II inhibitor commonly used in liver cancer treatment,<sup>3</sup> also has the fortuitous property of natural fluorescence. Polymer millirods containing doxorubicin were

implanted in nonablated and RF ablated rat livers.<sup>90</sup> Liver tissues were removed at various times after implantation, and local doxorubicin concentrations were determined by measuring the fluorescence of the extracted slices. Average doxorubicin concentrations at time points ranging from 1 h to 4 days after implant placement were used to estimate the transport properties of liver tissues within the framework of a theoretical model of drug distribution as described in the Overview of Drug Delivery Goals Section.<sup>58</sup> The resulting estimates are shown in Table 1. These studies established the baseline transport properties of doxorubicin in normal rat liver as well as

**Table 1.** Doxorubicin Transport Properties in Rat Liver

	Normal Liver	Ablated Liver
Apparent diffusion, $D^*$ , ( $\text{cm}^2 \cdot \text{s}^{-1}$ )	$6.7 \times 10^{-7}$	$1.1 \times 10^{-7}$
Apparent elimination, $\gamma^*$ , ( $\text{cm}^2 \cdot \text{s}^{-1}$ )	$9.6 \times 10^{-4}$	n/a

how ablation modifies them. Ablation reduced the diffusion coefficient, perhaps by destroying cell structure and making more sites available for drug binding. Even more notably, ablation virtually abolished elimination, which is sensible since RF ablation might be expected to reduce elimination both due to metabolism in cells (by killing them) and perfusion related losses (by coagulating and destroying blood vessels). This reduction in drug elimination can largely explain why drug penetration distances and retention were higher in ablated liver tissue.

In summary, techniques for measuring local drug concentrations surrounding implants are fundamentally important for the development of a local drug delivery system for tumors. Many methods exist for measuring drug concentrations, each with advantages and disadvantages, and it is likely that a combination of methods provide the best overall information about drug delivery. After obtaining local drug concentrations, they can be compared empirically to determine qualitative differences in delivery or interpreted through the use of a model to obtain quantitative transport information. Both sets of data can then be used to modify implant properties to provide the best drug coverage to the tumor.

### Controlling Drug Release and Local Pharmacokinetics from Polymer Implants

Development of techniques to monitor local drug pharmacokinetics allows for the design and assessment of different implant types. As described in the Overview of Drug Delivery Goals Section, an ideal implant should provide a rapid ascent to the therapeutic concentration and maintenance of this dose for as long as possible. The first generation polymer millirod provided rapid release of a drug mimic, largely within the first few days.<sup>65</sup> However, through modification of the implant design it is possible to customize the delivery profile of the implants. Consequently, local drug concentrations arising around the implants can be compared and evaluated based on overall tissue drug exposure.

Several modifications to the initial compression-heat molded millirods can either prolong drug release or change the timing of the released dose. One modification is the addition of a semi-permeable membrane around the outside of the implant, which can be made either by wrapping the cylindrical device with a membrane<sup>63</sup> or by dip

coating the implant.<sup>64</sup> Using these methods, polymer membranes containing NaCl (10–50% w/w) or poly(ethylene oxide) (PEO) (5–20% w/w) were placed around monolithic millirods. When placed in an aqueous environment, the water-soluble component of the outer membrane rapidly dissolved, leaving a semi-permeable membrane with porosity that could be modulated by controlling the water-soluble fraction. These membrane-encased millirods substantially prolonged the drug release from the resulting implants over a period as long as 5 weeks.<sup>63,64</sup>

By further modifying the polymer millirods, it is possible to create an implant that adds an additional burst dose to the millirods with sustained drug release. As discussed in the Overview of Drug Delivery Goals Section, the tissue surrounding a sustained release implant may not reach the therapeutic concentration for some time, delaying the onset of action of the drug. To accelerate the rise to the therapeutic concentration, a burst dose can be added to the implant to act as a loading dose. Dual-release implants combining the benefits of a drug burst followed by sustained release were then created by supplementing the implant with two drug coatings.<sup>58</sup> Monolithic millirod implants were first created by compression molding followed by the addition of two subsequent coatings. To sustain the release of drug from this implant, it was dip coated with a layer of PLA/PEG as described above. Then, a second coating consisting of doxorubicin and PEO was added to provide an additional burst dose. The total burst dose of drug could be controlled by applying multiple coatings to increase the thickness of the burst layer. The resulting implants, termed dual-release millirods, released a burst dose of doxorubicin followed by a sustained dose of doxorubicin for as long as 10 days.<sup>58</sup> In this manner, polymer millirods that could release doxorubicin into tumors with different dose timings were created.

To evaluate the differences in local drug distribution generated by different implant types, these burst, sustained, and dual-release millirod formulations were tested *in vivo*.<sup>64</sup> In the rat model, liver tissue was ablated for 2 min at 90°C to create an ablation region 8–10 mm in diameter. Subsequently, polymer millirods of each type were placed in the ablation needle tract and sutured into place. At specified time points, the rats were euthanized, and the polymer implants and surrounding liver tissue were extracted. Doxorubicin remaining in the implant was quantified by an

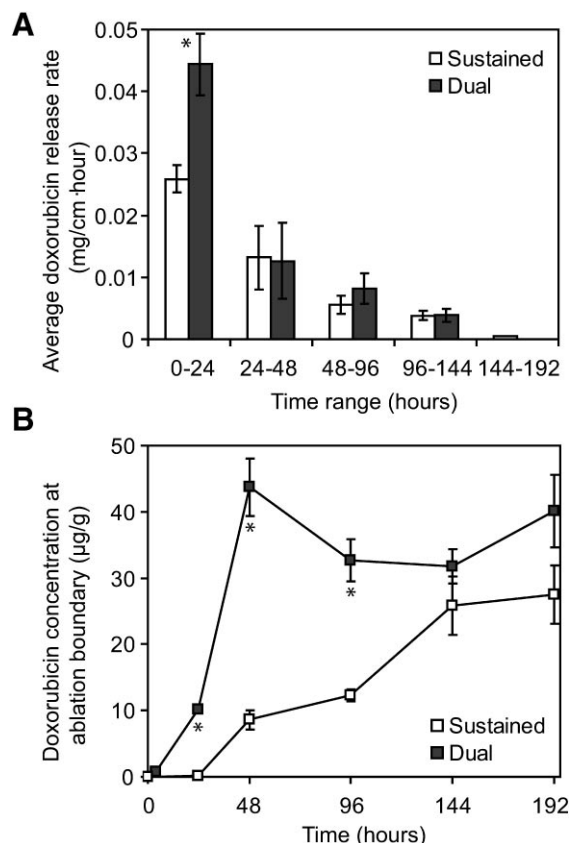


**Figure 5.** In vivo relationship between drug release rate and local tissue concentrations. A: Average rate of drug release from two implant formulations in vivo in ablated rat livers. B: Doxorubicin concentration at the outer edge of the ablated region for the same two implant formulations. Adapted from Reference<sup>64</sup> with permission.

extraction procedure and used to calculate average release rates, which are shown in Figure 5A. As expected, the dual-release implants released a higher amount of drug in the first 24 h,

but after this time the drug release rates were not statistically different. Tissue doxorubicin concentrations were determined using fluorescence scanning of sliced tissues, and the doxorubicin concentration at the outer ablation boundary is shown in Figure 5B. The dual-release implants provided a more rapid ascent to therapeutically relevant concentrations that was statistically different from the sustained-release implants. The similarity between the experimental results and the desired theoretical profiles shown in Figure 1 (panel 2, curves A and C) is notable. More detailed fluorescent images of tissues that confirm this finding are shown in Figure 6. Dual-release implants led to local doxorubicin concentrations as high as 1000  $\mu\text{g/g}$  within 1 day, while it took nearly 4 days for the drug distributions around the sustained implant to reach this extent. This study established that differences in implant formulation could have a substantial impact on local drug concentrations.

#### Controlling Host Tissue Response in Local Drug Therapy

Histology studies of treated tissue from ablated livers were performed to provide a more detailed understanding of the effect of changing tissue properties on drug transport.<sup>75</sup> Ablated rat livers were treated with doxorubicin-containing polymer implants, and tissues were subsequently removed at time points ranging from 1 h to 8 days after ablation. Throughout the first 4 days after ablation, an area of coagulation necrosis surrounding the implant was gradually infiltrated by inflammatory cells, particularly neutrophils and

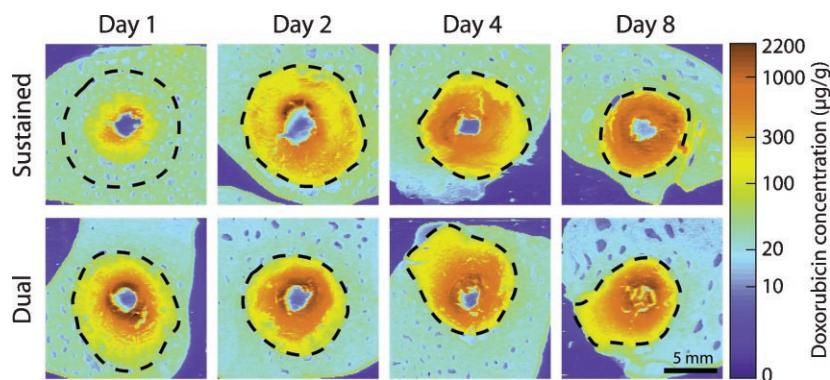


**Figure 6.** Fluorescence imaging comparing the rate of local doxorubicin accumulation due to two implant formulations (sustained-release and dual-release millirod) in ablated liver over 8 days. The dotted line is the ablation boundary, and the scale bar is 5 mm. Adapted from Reference<sup>64</sup> with permission.

monocytes. By 8 days after ablation, fibroblasts and the formation of a dense, collagenous fibrous capsule were evident at the ablation boundary. Furthermore, it was found that doxorubicin concentrations leading up to the fibrous capsule were high but dropped precipitously in the nascent fibrous capsule. From these results, it appeared that the wound healing response after ablation could have a major role in drug diffusion, acting as a barrier to transport outside the ablation region.<sup>75</sup> This finding reiterates the importance of considering the tissue surrounding the implant not as a static environment, but instead as a dynamic milieu that can ultimately affect the success of the treatment itself.

Since the tissue surrounding the implant has a large impact on the efficacy of drug therapy, one strategy to overcome this is to modify the response of the surrounding tissue in a way that favors effective drug dispersion. One way to modify the properties of ablated tissue is to moderate the ensuing inflammatory response with an anti-inflammatory agent. To test this hypothesis, the potent corticosteroid dexamethasone (DEX) was loaded into PLGA millirod implants.<sup>91</sup> To facilitate the subsequent release of DEX, a highly hydrophobic drug, a more water soluble DEX formulation complexed with hydroxypropyl  $\beta$ -cyclodextrin (HP $\beta$ -CD) was incorporated in the implants. These implants were tested for their ability to reduce fibrous capsule formation following liver ablation in rats. Histology with Masson's trichrome stain showed that the DEX-impregnated implants drastically suppressed the thickness of the collagen fibrous boundary compared to a control ablation treatment (Fig. 7). The average thickness of the fibrous capsule was  $0.04 \pm 0.01$  mm in subjects receiving a DEX implant, reduced both compared to a control ablation ( $0.29 \pm 0.08$  mm) or ablation followed by an IP DEX injection ( $0.26 \pm 0.07$  mm).<sup>91</sup>

In addition to enhancing drug delivery by reducing fibrous capsule formation, DEX administration after ablation may have other beneficial effects as well as some disadvantages. DEX is expected to reduce chemokine and growth factor production and angiogenic processes that have been implicated in tumor growth and recurrence after ablation.<sup>92-94</sup> At least one report has suggested that liver tumor recurrence after ablation is potentiated by inflammation,<sup>60</sup> which may allow DEX to improve the primary outcome of ablation. On the other hand, the inflammatory state of the tissue following ablation may con-

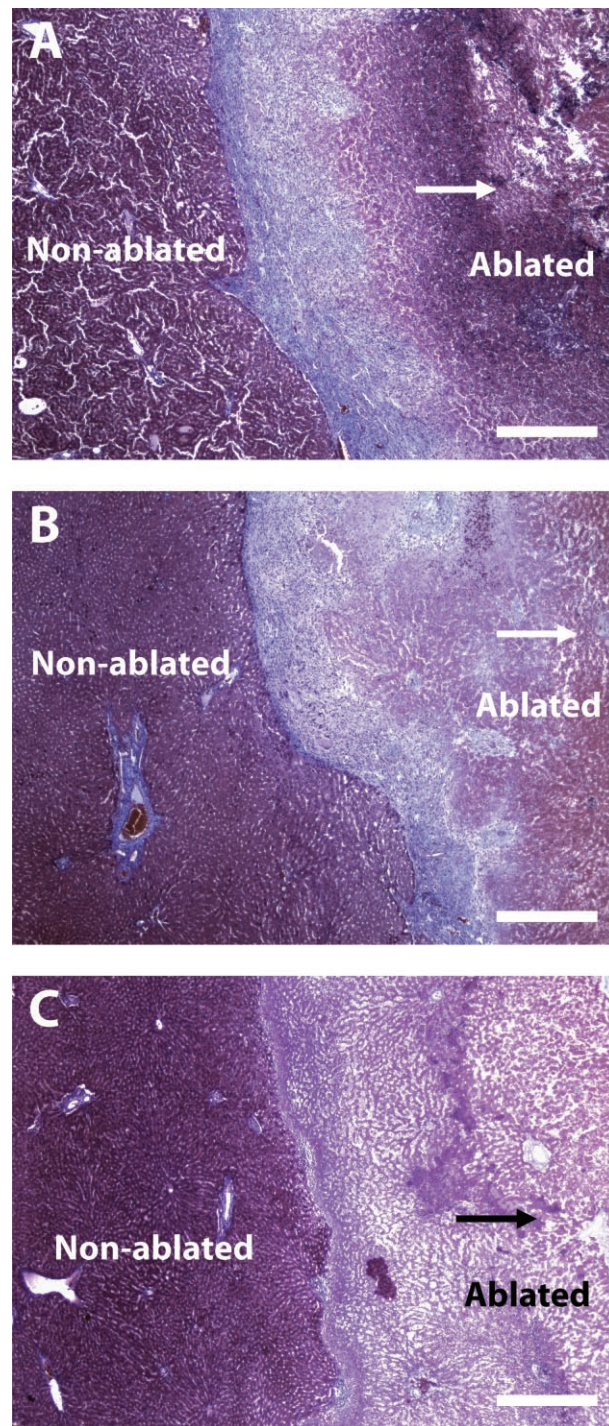


**Figure 7.** Masson's trichrome stained histology images of ablated liver samples 8 days after RF ablation and millirod implantation. A: Ablated liver receiving control PLGA millirod. B: Sample that received a control PLGA millirod and intraperitoneal (IP) injection of DEX. C: Ablated liver receiving DEX-loaded millirod. The arrows point to the center of the liver ablation/millirod implantation site. All scale bars are 0.5 mm. Adapted from Reference<sup>91</sup> with permission.

tribute to tumor destruction. In several reported studies, considerable damage has been found to occur following the initial thermal damage.<sup>95,96</sup> The authors have speculated that this progressive ablation damage could be a result of inflammatory activation or altered cytokine expression after ablation. If this process is interrupted, DEX could adversely affect the therapeutic outcome of ablation. This complication might be avoided by stopping revascularization using more specific drugs, such as a new class of drugs known as vascular disrupting agents.<sup>97</sup> Future study of implants containing multiple agents should allow for specific modification of tissue properties after ablation to achieve the most favorable tumor destruction with the combined treatment.

### Summary

Several different implant types were developed and evaluated in thermal ablation models of rat and rabbit livers. Two factors appeared to have a role in the extent of drug delivery: the rate of drug release and the properties of the surrounding tissue. Dual-release implants, consisting of two dip-coated layers, provided the fastest ascent to therapeutic concentrations and maintained local concentrations for at least 8 days. RF ablation, by destroying the surrounding vasculature, potentiated drug release into the surrounding tissue but may have ultimately restricted it by instigating the encapsulation of the ablated region within a thick fibrous shell. One approach, including DEX complexed with  $\beta$ -cyclodextrin in the implants, showed the potential to overcome this limitation. Overall, studies of drug release from implants demonstrated that PLGA implants are a versatile platform for drug delivery that is capable of different release kinetics and local pharmacokinetics following RF ablation.

## TREATMENT OF ANIMAL TUMOR MODELS

### Drug Distribution and Antitumor Efficacy from Liver Tumor Treatment with Polymer Implants

After extensive pharmacokinetic study of polymer millirods in normal livers, preliminary studies of drug distribution and treatment efficacy in tumor tissue were performed. One study assessed the use of implants alone for treatment and local control of small liver tumors;<sup>66</sup> the second study explored drug distribution and therapeutic effects

of an approach combining RF ablation followed by implant placement.<sup>67</sup> Both of these studies were performed using the rabbit VX2 model of liver carcinoma, which has been widely used in the assessment of new interventional therapies and is considered a realistic model of human HCC.<sup>98-100</sup> Together, these studies provide insight on the efficacy of liver tumor treatment with implantable polymer devices.

The first study established the use of polymer millirods as a standalone strategy for the treatment of small, unresectable liver cancers.<sup>66</sup> The primary goal of this work was to determine the drug distribution and the resulting treatment efficacy from using polymer implants to treat tumors smaller than 1 cm in diameter. Such a scenario might be encountered in humans in advanced HCC, when multiple small tumors might be found throughout the liver. In this case, surgery is often excluded because of insufficient liver function or the involvement of both liver lobes.<sup>101</sup> Small VX2 liver tumors (diameter = 8 mm) in New Zealand White rabbits were treated with the implantation of a burst-release doxorubicin millirod into the center of the tumor.<sup>66</sup> On a gross level, the implants demonstrated considerable tumor control at both time points, as tumors were 50% and 90% smaller than their respective controls. The treated tumors had a substantially different morphology than controls, showing considerable necrosis and cell damage. Drug penetration was seen at distances of 2.8 mm (day 4) and 1.3 mm (day 8) away from the implant. A plot of day 4 drug concentrations within the tumor as a function of distance from the implant is shown in Figure 8. Outside the tumor, drug concentrations dropped sharply and were below the detectable levels of drug. Furthermore, untreated tumor cells, which are likely to grow into recurrent tumors over time, were found outside the main tumor boundary. This study established that the polymer implants could be used to treat small tumors in a palliative or neoadjuvant role. Future studies with larger numbers of animal subjects will be further pursued to establish treatment success rates.

### Drug Distribution and Antitumor Efficacy from Combined Liver Tumor Treatment with Radiofrequency (RF) Ablation and Polymer Implants

After demonstrating the drug coverage and treatment effects provided by the implants alone,

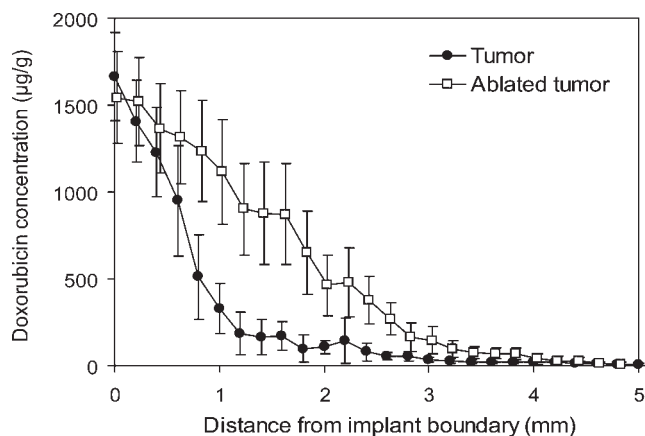


**Figure 8.** Average doxorubicin concentration in nonablated (●) or ablated (□) rabbit liver tumors as a function of distance from the implant 4 days after tumor treatment. Error bars show 95% confidence interval of the mean.

polymer millirods containing doxorubicin were tested as part of a combined liver cancer treatment.<sup>67</sup> The combined treatment consisted of RF ablation of the center of the tumor followed by the placement of a doxorubicin-containing implant. For liver tumor treatment, this approach has two distinct advantages. First, the RF treatment destroys the majority of the tumor mass, leading to a considerable reduction of viable tumor. Remnant tumor cells may also have increased susceptibility to drug because of their sublethal hyperthermia exposure. Second, RF ablation of the tumor mass facilitates drug distribution to greater distances from the implant, an effect established in earlier studies in normal liver.<sup>62,90</sup> This property should provide greater drug exposure to the tumor, and hence, a greater degree of success, than either treatment alone. Additionally, the combined treatment may be more clinically relevant, as combined treatments for human tumors are often regarded as more effective than single treatments.<sup>102</sup>

RF ablation followed by polymer implant placement was also tested in the VX2 liver carcinoma model in rabbits.<sup>67</sup> VX2 tumors of 1.1 cm in diameter were treated with RF ablation insufficient to destroy the entire tumor to mimic the human scenario in which a tumor is not completely treated. Following ablation, doxorubicin-containing polymer millirods were implanted into the ablation tract in the center of the tumors. Results from the combined treatment allowed for comparison of drug distribution properties between nonablated and ablated tumors. Radially averaged drug concentrations from the ablated tumors on day 4 are shown compared to those in

nonablated tumors in Figure 8. In both cases, drug concentrations in the center of the tumor are over 1000 µg/g at the implant tissue interface. However, the drug penetrates more deeply into ablated tumor tissues, providing greater drug coverage to the tumor 4 mm away from the implant boundary. Doxorubicin penetration distances in the ablated tumor tissue were found to be 3.7 mm on day 4 and 2.1 mm on day 8 (compared to 2.8 and 1.3 mm on day 4 and day 8 in nonablated tumors, respectively). Ablation almost tripled the total mass drug estimated to be in the tumor on day 4, increasing the value from  $210 \pm 120$  µg without ablation to  $590 \pm 300$  µg with ablation. The overall half-life of drug removal from the tumor volume was found to be  $2.0 \pm 0.1$  days, slower than the  $1.6 \pm 0.2$  days seen in nonablated tumor. These results support the conclusion that tumor ablation provides a reduction in drug elimination similar to that found in ablated normal liver, leading to greater penetration into the tumor tissue, and ultimately, greater coverage of the tumor with therapeutic drug values. Such data were qualitatively confirmed in images of drug distribution, which showed greater amounts of drug further from the tumor.

Gross pathological and histological observations after the combined treatment also allowed for preliminary assessment of the success of the combined treatment. The total area of coagulation necrosis and inflammatory tissue surrounding the ablated area was similar regardless of which type of implant was used. Totalling both time points, two out of seven animals treated with ablation and a control implant were found to have significant regions of residual tumor; similarly, two out of

seven animals treated with ablation and a doxorubicin implant had residual tumor. None of the animals (0/3) in the 8 day ablation plus implant group had areas of residual tumor, indicating a possible, although not statistically significant improvement in this group. Considerable knowledge on why the residual tumors remain untreated was determined from histological assessment. In the two residual tumors in the treatment group, areas of residual tumor began on average 4.1 mm away from the implant location, with 50% of the viable tumor found within 7.9 mm. Some residual tumor cells were found as far as 12.0 mm away from the implant. Comparison of tumor histology with fluorescence microscopy images provided further insight into why the treatment did not reach the entire tumor. Starting at day 4 and more considerable by day 8, fibrous capsule formation around the coagulated zone was evident. Fluorescence attributed to doxorubicin was seen up to the fibrous boundary on day 8, but little fluorescence was seen beyond this barrier, suggesting that collagen deposition in the boundary may have inhibited drug transport to untreated regions outside the ablated region (Fig. 9). The two main barriers to treatment success revealed by this study were drug penetration distance from the millirod implant and the formation of a fibrous barrier to drug transport.<sup>67</sup>

Together, the two studies of liver tumor treatment with polymer millirods provide several interesting findings about the probability of success for tumor treatment with implantable polymer devices. With doxorubicin containing millirods alone, relatively small lesions (<1.0 cm diameter) were controlled in terms of tumor size but may not have been ultimately cured because of the presence of residual cells around the periphery.<sup>66</sup> However, these results suggest that these implants may be successful in reducing tumor load and could serve as a palliative and life-prolonging strategy in patients who are not good candidates for surgical resection. For instance, patients with multiple small metastatic lesions to the liver could be treated with percutaneous, image-guided placement of an implant in each lesion. The study of the combined treatment was unable to elicit statistically significant values in likelihood of remnant viable tumor, but did reveal that fibrous capsule formation and therapeutic distance from the implant limit treatment of residual tumor.<sup>67</sup> Future studies can now address these issues, perhaps by including DEX in the implants to reduce fibrous capsule formation<sup>91</sup>

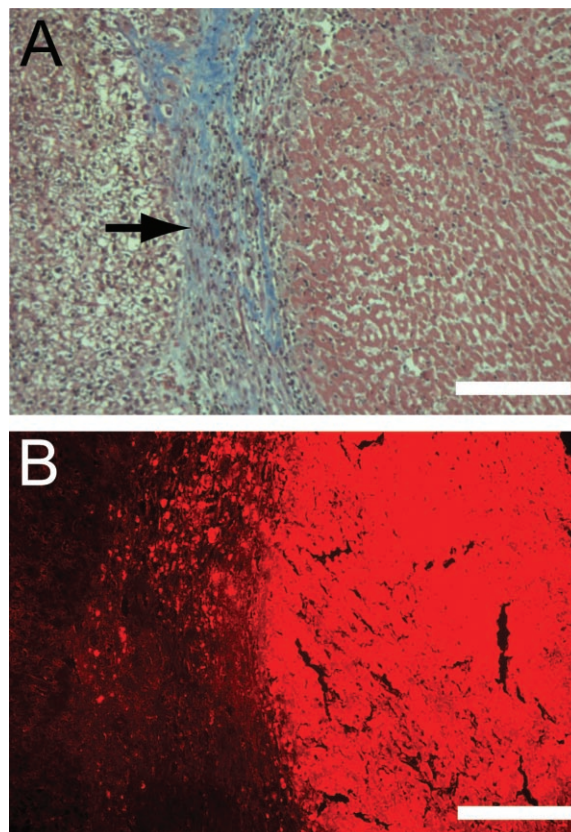


**Figure 9.** A: Masson's trichrome stained images of the ablation boundary 8 days after treatment. Ablated tissue is on the right and normal tissue on the left, with the boundary marked by the black arrow. A thick fibrous capsule was found at the ablation boundary. B: Fluorescent microscopy image of the matching regions showing doxorubicin accumulation just inside the ablation boundary. Scale bars are 200  $\mu\text{m}$ . Adapted from Reference<sup>67</sup> with permission.

and using multiple polymer millirods placed peripherally around the tumor to minimize the distance between the implants and risk areas for tumor recurrence.

### Three-Dimensional Modeling of Intratumoral Drug Delivery

Current research is focusing on the development of a 3-D finite element model to evaluate the effects of different implant designs and treatment strategies, such as the incorporation of an anti-inflammatory agent and the use of multiple millirods, on local cancer therapy. This approach limits the number of animal experiments and allows for rapid prototyping of different treatment

strategies. To model drug distribution into ablated tissues, transport properties of nonablated and ablated tumor were estimated. The resulting properties were then used to simulate drug distribution to ablated tumors with different types or arrangement of implants.

Tumor drug transport parameters were estimated by minimizing the error between a finite element solution to the transport mass balance equation and experimental data previously determined.<sup>66,67</sup> Nonablated tumor was found to have drug diffusion slightly less than normal liver tissue and elimination considerably less than normal liver tissue. Ablated tumor, on the other hand, had a doxorubicin diffusion rate higher than either normal liver or nonablated tumor. As was found in normal liver, ablation completely stopped drug elimination for 4 days, but due to reperfusion of the ablated tumor areas elimination returned to values similar to that in normal tumor between day 4 and day 8. This finding

indicates that much as in normal liver tissue, ablation provides a clear window for improved drug delivery that lasts 4–8 days.

The estimated tissue parameters were then used to simulate 3-D drug distribution profiles using multiple, peripherally placed implants to treat larger tumors. Exemplary scenarios using RF ablation followed by placement of 1 or 4 burst-release doxorubicin polymer millirods to treat a single tumor are shown in Figure 10. In this instance, a tumor measuring 2 cm in diameter has been treated with RF ablation insufficient to treat the entire tumor (1.8 cm ablation diameter). Drug transport was then simulated using a finite element solution to determine the drug concentrations throughout the tumor over an 8-day period. The resulting model predicted drug concentrations on day 8 are shown in Figure 10C,D. The drug distributions from four peripheral distributions show considerably higher drug concentrations, particularly in the nonablated tumor

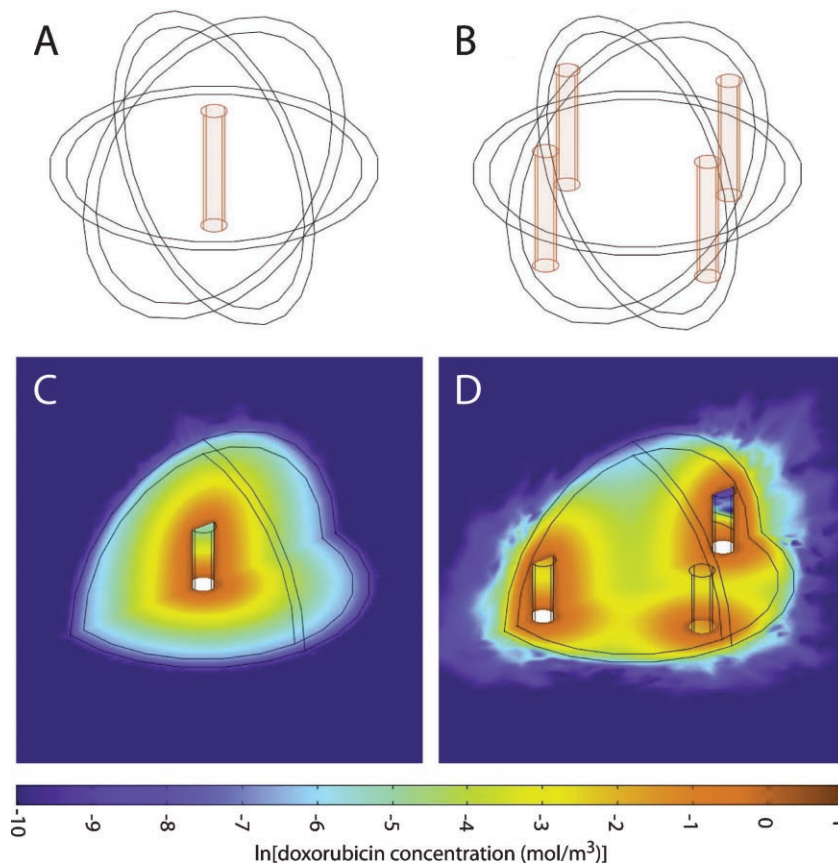


**Figure 10.** Simulated three-dimensional (3-D) geometry of a 2 cm diameter tumor containing a central RF ablated region of diameter 1.8 cm and treated with either one central implant (A) or four peripheral implants at a radius of 0.7 cm from the tumor center (B). Model predicted doxorubicin concentrations on day 8 for the single implant (C) and four implant (D) scenarios.



around the periphery of the lesion, where the tumor is most likely to recur. The four peripherally placed implants maintained the entire tumor volume at greater than two times the therapeutic concentration ( $>12.8 \mu\text{g/g}$ ) for 74 h, while the single implant never reached 100% tumor coverage during the simulated 8 days. These findings indicate that a multiple implant strategy may be advantageous over a single, centrally placed implant. However, this strategy could be limited by the ability of a physician to easily place multiple solid implants into a tumor. An alternative method is to use an injectable polymer gel that forms a solid depot *in situ*. The advantage of this strategy is that these depots can be injected as a liquid through a smaller needle, allowing for easier administration of drug in multiple positions. Several types of *in situ* forming implants are available, with their precipitation triggered by pH,<sup>103</sup> temperature,<sup>104</sup> or solvent exchange.<sup>47</sup> Future studies could be used to establish the benefits of using one of these delivery systems along with RF ablation.

Using drug distribution simulations, many different treatments can be rapidly compared to determine which has the maximum likelihood of success. Future extensions to this model can be used to predict how implants with different release profiles, such as dual-release doxorubicin implants, could improve tumor coverage. Additionally, the model will be able to evaluate how other changes to implant design that modify tissue properties, such as including DEX within the implants, can affect drug distribution in the tumors. Ultimately, a drug transport model may be used as part of a comprehensive treatment planning tool. Image-based data obtained from CT or MRI could be used to determine tumor geometry. Subsequently, ablation treatment could be planned using a thermal damage model,<sup>105</sup> after which drug coverage in the ablated tumor could be predicted using this 3-D finite element model. Using a computational tool to plan combined treatment would allow assessment of the best ways to treat complex lesions and extension of the findings from smaller tumors already reported into larger, more clinically relevant tumor models.

## CONCLUSIONS AND FUTURE OUTLOOK

Conventional systemic chemotherapy for tumors is restricted by lack of tumor specificity and severe

side effects associated with intrinsic drug toxicity.<sup>5-7</sup> With the emergence of minimally invasive, image-guided interventional technology, tumor chemotherapy is at the threshold of a major breakthrough because of such technological advances in targeting strategies that overcome the previous limitations. Tumor-directed therapies, such as focal ablation and locoregional chemotherapy, are being developed to increase the specificity of tumor destruction and reduce undesired side effects. Intratumoral implants reduce systemic drug exposure by using image-guided placement directly into the target region, thus delivering the entire drug dose with reduced systemic exposure. The key consideration with intratumoral chemotherapy is to design an implant system that provides optimal drug distribution and therefore maximal tumor destruction.

Polymer millirod implants were specifically designed to treat unresectable liver tumors in conjunction with RF ablation. Implants with different drug release rates have been developed and extensively studied in both nonablated and ablated liver tissues, where they effectively delivered drugs into the surrounding tissue. Particularly, dual-release implants combining a burst of drug release with sustained drug release maximized drug coverage in the ablated region.<sup>64</sup> Modeling of tissue properties using a pharmacokinetic transport model emphasized the importance of tumor pretreatment with RF ablation, which facilitated drug delivery to tissues further away from the implant by preventing drug elimination. Polymer millirods were further tested in a rabbit model of HCC. Tumor control was achieved within a limited distance from the implant, but several of the treated animals had regions of viable tumor just beyond the boundary of the ablation. The success of the tumor treatment appeared to be limited by two factors: drug transport distance from the implant and the formation of a fibrous capsule that restricted drug transport.

The future of polymer millirods for tumor treatment depends on optimizing drug delivery efficiency to the tumor periphery. One way of achieving this goal is to include an anti-inflammatory agent and doxorubicin in a single implant. DEX-containing polymer millirods have already been shown to prevent fibrous capsule formation and decrease new blood vessel formation after ablation.<sup>91</sup> These effects should promote drug delivery by increasing doxorubicin diffusion

and reducing elimination. Another anticipated improvement is placing multiple implants around the periphery of a larger tumor to improve the probability of treatment success. Placing implants closer to the boundary increases the likelihood of drug exposure at and beyond the ablation periphery, where recurrence is most likely to occur. The focus of a multiple implant strategy will be maximizing drug coverage of the tumor periphery while maintaining a reasonable and safe number of implants and total drug dose. 3-D modeling will be an essential tool for rapidly evaluating different treatment protocols as well as gaining mechanistic insights to optimize dosage regimen design. The integrated modeling and experimental approach should greatly assist the clinical translation of polymer implants as a viable option for locoregional chemotherapy of unresectable tumors.

#### ACKNOWLEDGMENTS

This work was supported by the NIH grant R01 CA090696 to JG. BW is supported by a DOD predoctoral fellowship BC043453 and the NIH grant T32 GM07250 to the Case Western Reserve University Medical Scientist Training Program. EB is supported by a NIH minority supplement. This is manuscript CSCNP009 from the "Cell Stress and Cancer Nanomedicine" program in the Simmons Comprehensive Cancer Center at UT Southwestern Medical Center at Dallas.

#### REFERENCES

1. Jemal A, Siegel R, Ward E, Murray T, Xu J, Smigal C, Thun MJ. 2006. Cancer statistics, 2006. *CA Cancer J Clin* 56:106–130.
2. Bentrem DJ, Dematteo RP, Blumgart LH. 2005. Surgical therapy for metastatic disease to the liver. *Annu Rev Med* 56:139–156.
3. Leung TW, Johnson PJ. 2001. Systemic therapy for hepatocellular carcinoma. *Semin Oncol* 28:514–520.
4. Geller DA, Tsung A, Marsh JW, Dvorchik I, Gambin TC, Carr BI. 2006. Outcome of 1000 liver cancer patients evaluated at the UPMC Liver Cancer Center. *J Gastrointest Surg* 10:63–68.
5. Dowell JA, Sancho AR, Anand D, Wolf W. 2000. Noninvasive measurements for studying the tumoral pharmacokinetics of platinum anticancer drugs in solid tumors. *Adv Drug Deliv Rev* 41:111–126.
6. Crawford J, Dale DC, Lyman GH. 2004. Chemotherapy-induced neutropenia: Risks, consequences, and new directions for its management. *Cancer* 100:228–237.
7. Wallace KB. 2003. Doxorubicin-induced cardiac mitochondrionopathy. *Pharmacol Toxicol* 93:105–115.
8. El-Kareh AW, Secomb TW. 2000. A mathematical model for comparison of bolus injection, continuous infusion, and liposomal delivery of doxorubicin to tumor cells. *Neoplasia* 2:325–338.
9. Gillams AR. 2005. Image guided tumour ablation. *Cancer Imaging* 5:103–109.
10. Barnett CC, Jr., Curley SA. 2001. Ablative techniques for hepatocellular carcinoma. *Semin Oncol* 28:487–496.
11. Goldberg SN. 2001. Radiofrequency tumor ablation: Principles and techniques. *Eur J Ultrasound* 13:129–147.
12. Vogl TJ, Mack MG, Muller PK, Straub R, Engelmann K, Eichler K. 1999. Interstitial therapy. *Eur Radiol* 9:1479–1487.
13. Han KR, Beldegrun AS. 2004. Third-generation cryosurgery for primary and recurrent prostate cancer. *BJU Int* 93:14–18.
14. Dale PS, Souza JW, Brewer DA. 1998. Cryosurgical ablation of unresectable hepatic metastases. *J Surg Oncol* 68:242–245.
15. Livraghi T, Benedini V, Lazzaroni S, Meloni F, Torzilli G, Vettori C. 1998. Long term results of single session percutaneous ethanol injection in patients with large hepatocellular carcinoma. *Cancer* 83:48–57.
16. Shah SS, Jacobs DL, Krasinkas AM, Furth EE, Itkin M, Clark TW. 2004. Percutaneous ablation of VX2 carcinoma-induced liver tumors with use of ethanol versus acetic acid: Pilot study in a rabbit model. *J Vasc Interv Radiol* 15:63–67.
17. Francica G, Marone G. 1999. Ultrasound-guided percutaneous treatment of hepatocellular carcinoma by radiofrequency hyperthermia with a 'cooled-tip needle'. A preliminary clinical experience. *Eur J Ultrasound* 9:145–153.
18. Merkle EM, Boll DT, Boaz T, Duerk JL, Chung YC, Jacobs GH, Varnes ME, Lewin JS. 1999. MRI-guided radiofrequency thermal ablation of implanted VX2 liver tumors in a rabbit model: Demonstration of feasibility at 0.2 T. *Magn Reson Med* 42:141–149.
19. Curley SA, Izzo F, Delrio P, Ellis LM, Granchi J, Vallone P, Fiore F, Pignata S, Daniele B, Cremona F. 1999. Radiofrequency ablation of unresectable primary and metastatic hepatic malignancies: Results in 123 patients. *Ann Surg* 230:1–8.
20. Varshney S, Sewkani A, Sharma S, Kapoor S, Naik S, Sharma A, Patel K. 2006. Radiofrequency ablation of unresectable pancreatic carcinoma: Feasibility, efficacy and safety. *JOP* 7:74–78.

21. Nguyen CL, Scott WJ, Goldberg M. 2006. Radio-frequency ablation of lung malignancies. *Ann Thorac Surg* 82:365–371.
22. Goldberg EP, Hadba AR, Almond BA, Marotta JS. 2002. Intratumoral cancer chemotherapy and immunotherapy: Opportunities for nonsystemic preoperative drug delivery. *J Pharm Pharmacol* 54:159–180.
23. Wientjes MG, Badalament RA, Au JL. 1996. Penetration of intravesical doxorubicin in human bladders. *Cancer Chemother Pharmacol* 37:539–546.
24. Seto T, Ushijima S, Yamamoto H, Ito K, Araki J, Inoue Y, Semba H, Ichinose Y. 2006. Intrapleural hypotonic cisplatin treatment for malignant pleural effusion in 80 patients with non-small-cell lung cancer: A multi-institutional phase II trial. *Br J Cancer* 95:717–721.
25. Alberts DS, Delforge A. 2006. Maximizing the delivery of intraperitoneal therapy while minimizing drug toxicity and maintaining quality of life. *Semin Oncol* 33:8–17.
26. Ramsey DE, Kernagis LY, Soulen MC, Geschwind JF. 2002. Chemoembolization of hepatocellular carcinoma. *J Vasc Interv Radiol* 13:S211–S221.
27. Kokudo N, Makuuchi M. 2004. Current role of portal vein embolization/hepatic artery chemoembolization. *Surg Clin North Am* 84:643–657.
28. Ramsey DE, Geschwind JF. 2002. Chemoembolization of hepatocellular carcinoma—what to tell the skeptics: Review and meta-analysis. *Tech Vasc Interv Radiol* 5:122–126.
29. Muller H, Hilger R. 2003. Curative and palliative aspects of regional chemotherapy in combination with surgery. *Support Care Cancer* 11:1–10.
30. Muller H. 2002. Combined regional and systemic chemotherapy for advanced and inoperable non-small cell lung cancer. *Eur J Surg Oncol* 28:165–171.
31. Hall WA, Sherr GT. 2006. Convection-enhanced delivery: Targeted toxin treatment of malignant glioma. *Neurosurg Focus* 20:E10.
32. Raghavan R, Brady ML, Rodriguez-Ponce MI, Hartlep A, Pedain C, Sampson JH. 2006. Convection-enhanced delivery of therapeutics for brain disease, and its optimization. *Neurosurg Focus* 20: E12.
33. Mardor Y, Roth Y, Lidar Z, Jonas T, Pfeffer R, Maier SE, Faibel M, Nass D, Hadani M, Orenstein A, Cohen JS, Ram Z. 2001. Monitoring response to convection-enhanced taxol delivery in brain tumor patients using diffusion-weighted magnetic resonance imaging. *Cancer Res* 61: 4971–4973.
34. Sampson JH, Akabani G, Friedman AH, Bigner D, Kunwar S, Berger MS, Bankiewicz KS. 2006. Comparison of intratumoral bolus injection and convection-enhanced delivery of radiolabeled anti-tenascin monoclonal antibodies. *Neurosurg Focus* 20:E14.
35. Celikoglu SI, Celikoglu F, Goldberg EP. 2006. Endobronchial intratumoral chemotherapy (EITC) followed by surgery in early non-small cell lung cancer with polypoid growth causing erroneous impression of advanced disease. *Lung Cancer* 54: 339–346.
36. Order SE, Siegel JA, Principato R, Zeiger LE, Johnson E, Lang P, Lustig R, Wallner PE. 1996. Selective tumor irradiation by infusional brachytherapy in nonresectable pancreatic cancer: A phase I study. *Int J Radiat Oncol Biol Phys* 36:1117–1126.
37. Mok TS, Kanekal S, Lin XR, Leung TW, Chan AT, Yeo W, Yu S, Chak K, Leavitt R, Johnson P. 2001. Pharmacokinetic study of intralesional cisplatin for the treatment of hepatocellular carcinoma. *Cancer* 91:2369–2377.
38. McGuire S, Yuan F. 2001. Quantitative analysis of intratumoral infusion of color molecules. *Am J Physiol Heart Circ Physiol* 281:H715–721.
39. McGuire S, Zaharoff D, Yuan F. 2006. Nonlinear dependence of hydraulic conductivity on tissue deformation during intratumoral infusion. *Ann Biomed Eng* 34:1173–1181.
40. Wang Y, Liu S, Li CY, Yuan F. 2005. A novel method for viral gene delivery in solid tumors. *Cancer Res* 65:7541–7545.
41. Wang Y, Yuan F. 2006. Delivery of viral vectors to tumor cells: Extracellular transport, systemic distribution, and strategies for improvement. *Ann Biomed Eng* 34:114–127.
42. Emerich DF, Snodgrass P, Lafreniere D, Dean RL, Salzberg H, Marsh J, Perdomo B, Arastu M, Winn SR, Bartus RT. 2002. Sustained release chemotherapeutic microspheres provide superior efficacy over systemic therapy and local bolus infusions. *Pharm Res* 19:1052–1060.
43. Menei P, Capelle L, Guyotat J, Fuentes S, Assaker R, Bataille B, Francois P, Dorwling-Carter D, Paquis P, Bauchet L, Parker F, Sabatier J, Faisant N, Benoit JP. 2005. Local and sustained delivery of 5-fluorouracil from biodegradable microspheres for the radiosensitization of malignant glioma: A randomized phase II trial. *Neurosurgery* 56:242–248; discussion 242–248.
44. Menei P, Jadaud E, Faisant N, Boisdron-Celle M, Michalak S, Fournier D, Delhaye M, Benoit JP. 2004. Stereotaxic implantation of 5-fluorouracil-releasing microspheres in malignant glioma. *Cancer* 100:405–410.
45. Arica B, Calis S, Kas H, Sargon M, Hincal A. 2002. 5-Fluorouracil encapsulated alginate beads for the treatment of breast cancer. *Int J Pharm* 242:267–269.
46. Almond BA, Hadba AR, Freeman ST, Cuevas BJ, York AM, Detrisac CJ, Goldberg EP. 2003. Efficacy

- of mitoxantrone-loaded albumin microspheres for intratumoral chemotherapy of breast cancer. *J Control Release* 91:147–155.
47. Krupka TM, Weinberg BD, Ziats NP, Haaga JR, Exner AA. 2006. Injectable polymer depot combined with radiofrequency ablation for treatment of experimental carcinoma in rat. *Invest Radiol* 41: 890–897.
  48. Jackson JK, Gleave ME, Yago V, Beraldi E, Hunter WL, Burt HM. 2000. The suppression of human prostate tumor growth in mice by the intratumoral injection of a slow-release polymeric paste formulation of paclitaxel. *Cancer Res* 60:4146–4151.
  49. Vogl TJ, Engelmann K, Mack MG, Straub R, Zangos S, Eichler K, Hochmuth K, Orenberg E. 2002. CT-guided intratumoural administration of cisplatin/epinephrine gel for treatment of malignant liver tumours. *Br J Cancer* 86:524–529.
  50. Merrick GS, Wallner KE, Butler WM. 2003. Permanent interstitial brachytherapy for the management of carcinoma of the prostate gland. *J Urol* 169:1643–1652.
  51. Grimm P, Sylvester J. 2004. Advances in Brachytherapy. *Rev Urol* 6:S37–S48.
  52. Guerin C, Olivi A, Weingart JD, Lawson HC, Brem H. 2004. Recent advances in brain tumor therapy: Local intracerebral drug delivery by polymers. *Invest New Drugs* 22:27–37.
  53. Wang PP, Frazier J, Brem H. 2002. Local drug delivery to the brain. *Adv Drug Deliv Rev* 54:987–1013.
  54. Brem H, Gabikian P. 2001. Biodegradable polymer implants to treat brain tumors. *J Control Release* 74:63–67.
  55. Fleming AB, Saltzman WM. 2002. Pharmacokinetics of the carmustine implant. *Clin Pharmacokinetics* 41:403–419.
  56. Strasser JF, Fung LK, Eller S, Grossman SA, Saltzman WM. 1995. Distribution of 1,3-bis(2-chloroethyl)-1-nitrosourea and tracers in the rabbit brain after interstitial delivery by biodegradable polymer implants. *J Pharmacol Exp Ther* 275:1647–1655.
  57. Westphal M, Ram Z, Riddle V, Hilt D, Bortey E. 2006. Gliadel wafer in initial surgery for malignant glioma: Long-term follow-up of a multicenter controlled trial. *Acta Neurochir (Wien)* 148:269–275; discussion 275.
  58. Qian F, Saidel GM, Sutton DM, Exner A, Gao J. 2002. Combined modeling and experimental approach for the development of dual-release polymer millirods. *J Control Release* 83:427–435.
  59. Chu G. 1994. Cellular responses to cisplatin. The roles of DNA-binding proteins and DNA repair. *J Biol Chem* 269:787–790.
  60. Harrison LE, Koneru B, Baramipour P, Fisher A, Barone A, Wilson D, Dela Torre A, Cho KC, Contractor D, Korogodsky M. 2003. Locoregional recurrences are frequent after radiofrequency ablation for hepatocellular carcinoma. *J Am Coll Surg* 197:759–764.
  61. Yu HC, Cheng JS, Lai KH, Lin CP, Lo GH, Lin CK, Hsu PI, Chan HH, Lo CC, Tsai WL, Chen WC. 2005. Factors for early tumor recurrence of single small hepatocellular carcinoma after percutaneous radiofrequency ablation therapy. *World J Gastroenterol* 11:1439–1444.
  62. Szymanski-Exner A, Gallacher A, Stowe NT, Weinberg B, Haaga JR, Gao J. 2003. Local carboplatin delivery and tissue distribution in livers after radiofrequency ablation. *J Biomed Mater Res* 67A:510–516.
  63. Qian F, Nasongkla N, Gao J. 2002. Membrane-encased polymer millirods for sustained release of 5-fluorouracil. *J Biomed Mater Res* 61:203–211.
  64. Qian F, Stowe N, Saidel GM, Gao J. 2004. Comparison of doxorubicin concentration profiles in radiofrequency-ablated rat livers from sustained- and dual-release PLGA millirods. *Pharm Res* 21: 394–399.
  65. Qian F, Szymanski A, Gao J. 2001. Fabrication and characterization of controlled release poly(D, L-lactide-co-glycolide) millirods. *J Biomed Mater Res* 55:512–522.
  66. Weinberg BD, Ai H, Blanco E, Anderson JM, Gao J. 2006. Antitumor efficacy and local distribution of doxorubicin via intratumoral delivery from polymer millirods. *J Biomed Mater Res A* 81:161–170.
  67. Weinberg BD, Blanco E, Lempka SF, Anderson JM, Exner AA, Gao J. 2006. Combined radiofrequency ablation and doxorubicin-eluting polymer implants for liver cancer treatment. *J Biomed Mater Res A* 81:205–213.
  68. Jain RK. 1999. Transport of molecules, particles, and cells in solid tumors. *Annu Rev Biomed Eng* 1:241–263.
  69. Sinek J, Frieboes H, Zheng X, Cristini V. 2004. Two-dimensional chemotherapy simulations demonstrate fundamental transport and tumor response limitations involving nanoparticles. *Biomed Microdevices* 6:297–309.
  70. Jain RK. 2001. Delivery of molecular and cellular medicine to solid tumors. *Adv Drug Deliv Rev* 46:149–168.
  71. Kalyanasundaram S, Calhoun VD, Leong KW. 1997. A finite element model for predicting the distribution of drugs delivered intracranially to the brain. *Am J Physiol* 273:R1810–R1821.
  72. Longley DB, Harkin DP, Johnston PG. 2003. 5-fluorouracil: Mechanisms of action and clinical strategies. *Nat Rev Cancer* 3:330–338.
  73. Tanner B, Hengstler JG, Dietrich B, Henrich M, Steinberg P, Weikel W, Meinert R, Kaina B, Oesch F, Knapstein PG. 1997. Glutathione, glutathione

- S-transferase alpha and pi, and aldehyde dehydrogenase content in relationship to drug resistance in ovarian cancer. *Gynecol Oncol* 65: 54–62.
74. Au JL, Jang SH, Wientjes MG. 2002. Clinical aspects of drug delivery to tumors. *J Control Release* 78:81–95.
  75. Blanco E, Qian F, Weinberg B, Stowe N, Anderson JM, Gao J. 2004. Effect of fibrous capsule formation on doxorubicin distribution in radiofrequency ablated rat livers. *J Biomed Mater Res A* 69:398–406.
  76. Wang CC, Li J, Teo CS, Lee T. 1999. The delivery of BCNU to brain tumors. *J Control Release* 61:21–41.
  77. Haaga JR, Exner AA, Wang Y, Stowe NT, Tarcha PJ. 2005. Combined tumor therapy by using radiofrequency ablation and 5-FU-laden polymer implants: Evaluation in rats and rabbits. *Radiology* 237:911–918.
  78. Zheng JH, Chen CT, Au JL, Wientjes MG. 2001. Time- and concentration-dependent penetration of doxorubicin in prostate tumors. *AAPS PharmSci* 3:E15.
  79. Lu Y, Segal E, Leamon CP, Low PS. 2004. Folate receptor-targeted immunotherapy of cancer: Mechanism and therapeutic potential. *Adv Drug Deliv Rev* 56:1161–1176.
  80. Roselt P, Meikle S, Kassiou M. 2004. The role of positron emission tomography in the discovery and development of new drugs; as studied in laboratory animals. *Eur J Drug Metab Pharmacokinet* 29:1–6.
  81. Moon WK, Lin Y, O'Loughlin T, Tang Y, Kim DE, Weissleder R, Tung CH. 2003. Enhanced tumor detection using a folate receptor-targeted near-infrared fluorochrome conjugate. *Bioconjug Chem* 14:539–545.
  82. Ntziachristos V. 2006. Fluorescence molecular imaging. *Annu Rev Biomed Eng* 8:1–33.
  83. Weinmann HJ, Ebert W, Misselwitz B, Schmitt-Willich H. 2003. Tissue-specific MR contrast agents. *Eur J Radiol* 46:33–44.
  84. Ye F, Ke T, Jeong EK, Wang X, Sun Y, Johnson M, Lu ZR. 2006. Noninvasive visualization of in vivo drug delivery of poly(L-glutamic acid) using contrast-enhanced MRI. *Mol Pharm* 3: 507–515.
  85. Nasongkla N, Bey E, Ren J, Ai H, Khemtong C, Guthi JS, Chin SF, Sherry AD, Boothman DA, Gao J. 2006. Multifunctional polymeric micelles as cancer-targeted, MRI-ultrasensitive drug delivery systems. *Nano Lett* 6:2427–2430.
  86. Szymanski-Exner A, Stowe NT, Lazebnik RS, Salem K, Wilson DL, Haaga JR, Gao J. 2002. Noninvasive monitoring of local drug release in a rabbit radiofrequency (RF) ablation model using X-ray computed tomography. *J Control Release* 83:415–425.
  87. Szymanski-Exner A, Stowe NT, Salem K, Lazebnik R, Haaga JR, Wilson DL, Gao J. 2003. Non-invasive monitoring of local drug release using X-ray computed tomography: Optimization and in vitro/in vivo validation. *J Pharm Sci* 92:289–296.
  88. Exner AA, Weinberg BD, Stowe NT, Gallacher A, Wilson DL, Haaga JR, Gao J. 2004. Quantitative computed tomography analysis of local chemotherapy in liver tissue after radiofrequency ablation. *Acad Radiol* 11:1326–1336.
  89. Gao J, Qian F, Szymanski-Exner A, Stowe N, Haaga J. 2002. In vivo drug distribution dynamics in thermoablated and normal rabbit livers from biodegradable polymers. *J Biomed Mater Res* 62:308–314.
  90. Qian F, Stowe N, Liu EH, Saidel GM, Gao J. 2003. Quantification of in vivo doxorubicin transport from PLGA millirods in thermoablated rat livers. *J Control Release* 91:157–166.
  91. Blanco E, Weinberg BD, Stowe NT, Anderson JM, Gao J. 2006. Local release of dexamethasone from polymer millirods effectively prevents fibrosis after radiofrequency ablation. *J Biomed Mater Res A* 76:174–182.
  92. Coussens LM, Werb Z. 2002. Inflammation and cancer. *Nature* 420:860–867.
  93. Raz A, Levine G, Khomiak Y. 2000. Acute local inflammation potentiates tumor growth in mice. *Cancer Lett* 148:115–120.
  94. Wang JM, Deng X, Gong W, Su S. 1998. Chemokines and their role in tumor growth and metastasis. *J Immunol Methods* 220:1–17.
  95. Nikfarjam M, Malcontenti-Wilson C, Christophi C. 2005. Focal hyperthermia produces progressive tumor necrosis independent of the initial thermal effects. *J Gastrointest Surg* 9:410–417.
  96. Nikfarjam M, Muralidharan V, Christophi C. 2005. Mechanisms of focal heat destruction of liver tumors. *J Surg Res* 127:208–223.
  97. Tozer GM, Kanthou C, Baguley BC. 2005. Disrupting tumour blood vessels. *Nat Rev Cancer* 5:423–435.
  98. Ramirez LH, Zhao Z, Rougier P, Bognel C, Dzodic R, Vassal G, Ardouin P, Gouyette A, Munck JN. 1996. Pharmacokinetics and antitumor effects of mitoxantrone after intratumoral or intraarterial hepatic administration in rabbits. *Cancer Chemother Pharmacol* 37:371–376.
  99. Yoon CJ, Chung JW, Park JH, Yoon YH, Lee JW, Jeong SY, Chung H. 2003. Transcatheter arterial chemoembolization with paclitaxel-lipiodol solution in rabbit VX2 liver tumor. *Radiology* 229: 126–131.
  100. Boehm T, Malich A, Goldberg SN, Hauff P, Reinhardt M, Reichenbach JR, Muller W, Fleck M, Seifert B, Kaiser WA. 2002. Radio-frequency ablation of VX2 rabbit tumors: Assessment of

- completeness of treatment by using contrast-enhanced harmonic power Doppler US. *Radiology* 225:815–821.
101. Kashef E, Roberts JP. 2001. Transplantation for hepatocellular carcinoma. *Semin Oncol* 28:497–502.
  102. Ashby LS, Ryken TC. 2006. Management of malignant glioma: Steady progress with multimodal approaches. *Neurosurg Focus* 20:E3.
  103. Shim WS, Kim JH, Kim K, Kim YS, Park RW, Kim IS, Kwon IC, Lee DS. 2007. pH- and temperature-sensitive, injectable, biodegradable block copolymer hydrogels as carriers for paclitaxel. *Int J Pharm* 331:11–18.
  104. Jeong B, Bae YH, Lee DS, Kim SW. 1997. Biodegradable block copolymers as injectable drug-delivery systems. *Nature* 388:860–862.
  105. Johnson PC, Saidel GM. 2002. Thermal model for fast simulation during magnetic resonance imaging guidance of radio frequency tumor ablation. *Ann Biomed Eng* 30:1152–1161.